Original Article

DOI: 10.5582/bst.2019.01190

Neuron loss and dysfunctionality in hippocampus explain aircraft noise induced working memory impairment: a resting-state fMRI study on military pilots

Huijuan Cheng[1,2,§], Guodong Sun[1,3,§], Mei Li[1], Minhong Yin[1], Hao Chen[1,2,*]

[1] *Lanzhou University Second Hospital, Lanzhou, Gansu, China;*
[2] *The Key Laboratory of the Digestive System Tumors of Gansu Province, Lanzhou, Gansu, China;*
[3] *The Regiment Medical Company, 96875 Army of PLA, Baoji, Shaanxi, China.*

Summary **Long-term aircraft noise exposure may cast a detrimental effect upon the working memory of military pilots, and the brain structural and functional bases of noise related cognitive impairment remains unclear. In this study, we enrolled 30 fighter jet pilots and 30 matched controls. The working memory performance of the subjects was measured with a neurobehavioral test battery including immediate verbal/visual memory and delayed verbal/visual memory tests. Structural MRI and resting-state functional magnetic resonance imaging (rs-fMRI) were utilized to quantify brain grey matter volumes (GMV), regional homogeneity (ReHo), amplitude of low-frequency fluctuation (ALFF) and fractional ALFF (fALFF) differences between the two groups. Furthermore, correlation analyses were performed to find the association between the neural imaging changes with individual neurobehavioral performance. The military pilots showed significantly lower accuracy in delayed verbal and visual memory tests in comparison to the controls, indicating a potential working memory deficit in this population. Structural MRI data and rs-fMRI data showed that the pilots displayed markedly decreased GMVs, ReHo and ALFF signals in the left hippocampus, suggesting neuron dysfunction of the hippocampus. Besides, ReHo and ALFF/fALFF analysis also revealed reduced ReHo in the left amygdala, left thalamus, left superior temporal gyrus and right superior/middle frontal gyrus, indicating disrupted local neural activity under chronic noise exposure. Furthermore, Spearman correlation analysis proved that the GMV and ReHo of left hippocampus were significantly associated with working memory accuracy. This study provided direct evidence of dysfunctional hippocampus serving as the structural and functional bases for neuropsychological impairment under aircraft noise exposure.**

Keywords: Aircraft noise, working memory, hippocampus, MRI

1. Introduction

The detrimental effects of aircraft noise on cognitive function and working memory are well documented (*1*). For instance, previous studies reported that aircraft noise may impair cognitive function of schoolchildren around airports, including recognition memory, attention and reading comprehension (*2*). Another study reported that nocturnal aircraft noise exposure induces significant delayed significant, linear impairments in reaction times (*3*). Compared with residents near airports, military pilots encounter more excessive aircraft noise while on duty. Noise levels generated by aircraft vary according to phase of flight as well as environmental factors, and ambient noise in the cockpit can reach as high as 80-120 dB along the flight. Previous studies have proved that ambient aircraft noise exposure injured hearing acuity of pilots and leads to hearing loss (*4*). Compared to the studies about hearing

Released online in J-STAGE as advance publication October 11, 2019.

[§]These authors contributed equally to this work.

**Address correspondence to:*
Dr. Hao Chen, The Key Laboratory of the Digestive System Tumors of Gansu Province, Lanzhou University Second Hospital, Lanzhou 730030, China.
E-mail: chenhao3996913@163.com

acuity, there are fewer studies on the cognitive and memory impairments associated with aircraft noise in the military pilot population.

Studies demonstrated that noise can lead to structural damages to the cochlea and hyperactivity in the central auditory pathway, including cochlear nucleus, inferior colliculus and auditory cortex at its traumatic levels (*5*). Besides, noise also triggers non-classical auditory-responsive brain areas (*e.g.* the lateral amygdala and striatum) and directly activates the emotion/fear system of the brain via the thalamus. In this way, noise can activate defense responses leading to activation of the hypothalamic–pituitary–adrenal (HPA) axis (*6*). Long-lasting activation of the HPA axis can lead to disturbed hormonal balance as well as morphometric and functional alteration of brain, which may be the potential mechanism of noise induced cognitive impairment (*7*). In a recent study in mice, chronic noise exposure adversely influenced the animals' behavior and brain structure. The noise stress caused HPA-axis hyperactivity, a reduction of size in the hippocampus, medial prefrontal cortex (mPFC), and amygdala, a reduced neuronal density in the mPFC and dentate gyrus (DG), and lower performance in all cognitive and motor tasks (*8*). Similarly, another study in mice revealed that noise may alter the long-term potentiation (LTP) and place cell activity in the hippocampus, and thus lead to spatial memory impairment (*9*). However, although a series of animal studies declared the brain morphometric with functional alteration under noise exposure, there's still a lack of direct human evidence of brain structural and functional bases of cognitive impairment.

In order to solve this problem, we focus on the military pilot population and try to reveal structural and functional alteration of the human brain under excessive aircraft noise exposure. Neuroimaging techniques, including anatomical T1-weighted MRI and resting-state functional MRI (rs-fMRI), allow us to accomplish this purpose. Anatomical T1-weighted MRI was routinely used for voxel-based morphology (VBM) to explore possible changes in grey matter volume (GMV); in turn, regional homogeneity (ReHo) analysis based on rs-fMRI can reflect the intrinsic functional organization and the endogenous neurophysiological process of the human brain, providing pertinent information on core mechanisms of neuropsychological disorders (*10*). We hypothesized that modified GMV and ReHo in certain brain regions will be revealed in comparison to those of the control population and these brain regions with differences may be associated with the working memory function of the subjects. To our knowledge, this is the first neuroimaging study comprehensively clarifing the potential cognitive and neuroimaging status in military pilots, which will help to elucidate the core mechanism of neuropsychological impairment under chronic aircraft noise exposure.

2. Materials and Methods

2.1. *Subjects*

30 male subjects in exposure group were randomly extracted from the 105 fighter jet pilots aged between 30-35 in an air force base in Gansu, China, while 30 male subjects in the control group were enrolled from the 429 military officers in an air force hospital in Gansu. All subjects in the two groups were matched by age, working life and education status. Excluded from the study were subjects who had a history of smoking and alcohol drinking, family history of neuropsychological diseases and exposure to audiological risk factors outside work (noise trauma, bomb, mine or other explosions, and use of firearms). For pilots in the exposure group, a Class-1 sound level meter (Brüel & Kjær, Denmark) was used to measure the equivalent continuous noise level in the cockpit of the fighter jet during the latest fight. The flight hours from the start of the pilot's working life were calculated by means of a questionnaire and a check on personal archives.

The protocol of this study was approved by the Ethics Committee of the Medical Faculty of Second Hospital of Lanzhou University (registry no. 2017A-074) and all study elements were conducted in accordance with ethical principles for medical research involving human subjects as defined in the Declaration of Helsinki. All subjects were fully aware of the study procedures and signed informed consent forms (ICFs).

2.2. *Working memory tests*

A neuropsychological test battery consisting of four computerized tests, were employed to assess the immediate verbal memory (IVBM), immediate visual memory (IVIM), delayed verbal memory (DVBM) and delayed visual memory (DVIM) of the subjects. All the verbal/visual memory tests were performed in the system of CNS Vital Signs (*http://www.cnsvs.com/*) (11,12).

2.3. *MRI image acquisition*

MRI were acquired using the General Electric Discovery MR750 3.0T systems (General Electric Co. Ltd., Connecticut, USA) in the Second Hospital of Lanzhou University. Standard T1-weighted 3D anatomical data were acquired using the 3D magnetization-prepared rapid gradient echo (3D MPRAGE) sequence (repetition time: 2530 ms; echo time: 3.5 ms; flip angle: 7°; field of view: 256 mm × 256 mm; matrix: 256 × 256; slice thickness: 1 mm; section gap: 0 mm; number of slices: 192, voxel size = 1 × 1 × 1 mm^3).

Rs-fMRI data were acquired with echo planar imaging (EPI) sequence (repetition time: 2000 ms;

echo time: 30 ms; flip angle: 90°; field of view: 220 mm × 220 mm; acquisition/reconstruction matrix: 128 × 128; slice thickness: 4 mm; section gap: 0.6 mm; number of slices: 30, scam time: 6min; voxel size = 3 × 3 × 3 mm^3) covering the entire brain. A custom-built head coil cushion and earplugs were used to minimize head motion and dampen scanner noise. During data acquisition, subjects were asked to remain alert with eyes closed and keep their head still.

2.4. *Structural MRI analysis*

Structural MRI data was analyzed by voxel-based morphometry (VBM) in Statistical Parametric Mapping software (SPM8, Wellcome Department of Cognitive Neurology, London, UK; *http://www.fil.ion.ucl.ac.uk/spm/*) in MATLAB R2014a (MathWorks Inc., Natick, MA, USA) (*13*). Data processing steps were performed according to Ashburner. We applied Diffeomorphic Anatomical Registration through Exponentiated Lie Algebra (DARTEL), which is implemented as a toolbox for SPM8 and enables the creation of a set of group-specific templates. Its performance on non-linear registration algorithms is better than that of other similar toolboxes. Brain images were segmented, normalized and modulated by using these templates. Registered images were then transformed to Montreal Neurological Institute (MNI) space, and finally, the normalized and modulated images were smoothed with a 6 mm full-width at half-maximum (FWHM) Gaussian kernel (*14,15*).

2.5. *Rs-fMRI preprocessing and analysis*

Rs-fMRI data pre-processing was then performed using the SPM8 and Data Processing Assistant for Resting-state fMRI Advanced (DPARSFA) tools. Prior to pre-processing, the first 10 volumes were discarded to reach a steady-state magnetization and allow participants to adapt to the scanning noise. For each subject, fMRI data were first adjusted for slice timing and head-motion (exclusion criteria: N 2.5 mm translation and/or N3.0° rotation). Then, the standard MNI template provided by SPM was further used for normalization with resampling to 3 mm × 3 mm × 3 mm voxels and spatially smoothed using a 4 mm × 4 mm × 4 mm full with a half-maximum Gaussian kernel. Next, a band-pass filter of 0.01 to 0.08 Hz was applied to the data in temporal frequency space to minimize low-frequency signal drift and high frequency variations due to cardiac and respiratory effects. In nuisance covariates regression, we selected the 6 head motion parameters, white matter signal, global mean signal, and cerebrospinal fluid signal as nuisance variables and regressed them out (*16,17*). The results are shown at $p < 0.05$ using false discovery rate (FDR) correction (with a combination of a threshold of $p < 0.001$ and a mini-mum cluster size of 65 voxels).

Voxel-based comparison of ReHo were conducted in Resting State fMRI Data Analysis Toolkit (REST) Version 2.0 (*http://restfmri.net/forum/REST_V2.0*). Computation of ReHo at resting state was performed as previously described. Briefly, Kendall's coefficient of concordance (KCC) for each voxel in the brain was calculated voxel-wise by applying a cluster size of 26 voxels. For standardization purposes, each individual ReHo map was divided by that subject's global mean brain KCC value to minimize inter-individual variability for statistical analysis within the whole-brain mask. Results are shown at $p < 0.05$ using AlphaSim correction (with a combination of a threshold of $p < 0.01$ and a mini- mum cluster size of 65 voxels) (*18,19*).

Using the preprocessed images, very low-frequency drift and high-frequency noise was first filtered (band-pass, 0.01~0.08Hz), then amplitude of low-frequency fluctuation (ALFF) were built according to standard procedures established by previous research (*20*). The filtered time series was transformed to the frequency domain using the fast Fourier transform (FFT) and the power spectrum was then obtained. The square root was calculated at each frequency of the power spectrum and taken as the ALFF. Furthermore, in order to eliminate physiological signals, fractional ALFF (fALFF) was also performed (*21*). Similar to ALFF, the square root was calculated at each frequency of the power spectrum. The sum of amplitude across 0.01-0.08 Hz was divided by that across the entire frequency range, *i.e.*, 0-0.25 Hz. Both the subject-level ALFF and fALFF were converted into a z-score map by subtracting the mean ALFF of the whole brain and dividing by the standard deviation (*22,23*). Results are shown at $p < 0.05$ using AlphaSim correction (with a combination of a threshold of $p < 0.01$ and a mini- mum cluster size of 65 voxels) (*18,19*).

2.6. Statistical analysis

Student *t* test was applied to assess differences of demographic and neurobehavioral parameters between the two groups. Spearman correlation coefficients were separately computed to examine correlations between GMV/ReHo and neuropsychological parameters. All statistical analyses were performed with R 3.1.3 (*https://www.r-project.org*). $p < 0.05$ was considered statistically significant.

3. Results

3.1. *Demographic information and noise exposure level*

Demographic information of the military pilots in the exposure group and controls are listed in Table 1. There were no significant difference between age, work lives and education status of the two groups. The flight hours

Table 1. Demographic information of the subjects in the exposure and control groups

Parameters	Exposure group (Military pilots of fighter jets) $n = 30$	Control group (Military officers in hospital) $n = 30$	t value	p value
Age (year)				
Mean (SD)	32.67 ± 1.19	33.07 ± 1.37	– 1.230	0.224
Range	30.1 – 34.4	30.6 – 34.9		
Working life (year)				
Mean (SD)	10.00 ± 1.72	10.37 ± 1.96	– 0.771	0.444
Range	7 – 12	7 – 14		
Education status (year)				
Mean (SD)	16.27 ± 0.69	16.07 ± 0.94	0.936	0.353
Range	15 – 18	15 – 19		

Table 2. Descriptive values (mean ± SD) and statistics of the working memory tests

Tests	Numbers of correct responses		t value	p value
	Exposure group	Control group		
IVBM	26.13 ± 2.65	26.40 ± 2.11	0.431	0.668
IVIM	22.67 ± 2.23	23.17 ± 2.23	0.868	0.389
DVBM*	24.60 ± 3.13	26.23 ± 2.70	2.166	0.034
DVIM**	19.00 ± 3.27	21.47 ± 3.25	2.933	0.005

IVBM, immediate verbal memory; IVIM, immediate visual memory; DVBM, delayed verbal memory; DVIM, delayed visual memory. *, $p < 0.05$; **, $p < 0.01$.

of the pilots in the exposure group were 840-1520 h, while the average equivalent continuous noise level in the cockpit was 108.6 ± 2.4 dB.

3.2. *Working memory measurements*

The results of the working memory tests are displayed in Table 2. There was no significant difference between the exposure and control group for the numbers of correct responses in IVBM and IVIM tests ($p = 0.668$ & 0.389, respectively). However, the numbers of correct responses in DVBM and DVIM tests were significantly less in the exposure group compared to control group ($p = 0.034$ & 0.005, respectively).

3.3. *VBM analysis of GMV changes*

Structural imaging analysis using VBM revealed brain structural differences between exposure and control group. Exposure group was observed to have less GMV in the left hippocampus, right middle frontal gyrus and right inferior parietal lobule compared with control group (t-test, $|t| > 3.02$, $p < 0.002$, $p < 0.05$ FDR corrected). What's more, exposure group was also found to have more GMV in the left caudate body. See details in Figure 1 and Table 3.

3.4. *ReHo analysis of rs-fMRI data*

Functional imaging analysis based on rs-fMRI was performed to investigate the ReHo differences between the two groups. Compared to control group, exposure group showed significantly lower ReHo values in the left amygdala, left hippocampus, left thalamus and right middle/superior frontal gyrus (t-test, $|t| > 2.70$, $p < 0.01$, AlphaSim corrected). In the meantime, exposure group showed higher ReHo values in the left cingulate and the right inferior temporal gyrus, compared to the control group. See details in Figure 2 and Table 4.

3.5. *ALFF/fALFF analysis of rs-fMRI data*

Furthermore, we used the ALFF/fALFF analysis based on rs-fMRI to examine neural activity changes after noise exposure. As shown in Table 5 and Figure 3, significantly lower ALFF signals were found in the left hippocampus, thalamus and the superior temporal gyrus, and significantly lower fALFF signals were observed in left middle temporal gyrus and left superior frontal gyrus, by which we confirmed that noise causes disrupted local neural activity in these regions, exactly. What's more, our analysis also showed significantly increased ALFF signals in the postcentral gyrus (Brodmann area 6, 22, 42, 43) and posterior cerebellum lobe. See details in Figure 3 and Table 5.

3.6. *Correlation between neurobehavioral performance and neuroimaging parameters*

In order to understand the effects of aircraft noise exposure on brain structure and function, we conducted correlation analyses between the performance of working memory tests and the corresponding GMV and ReHo of brain regions with significant differences between the two groups. As a result, the GMV of left hippocampus showed significantly positive associations with the DVIM accuracy (Figure 4A, $p = 0.0278$, $r = 0.3122$), while the ReHo of left hippocampus were

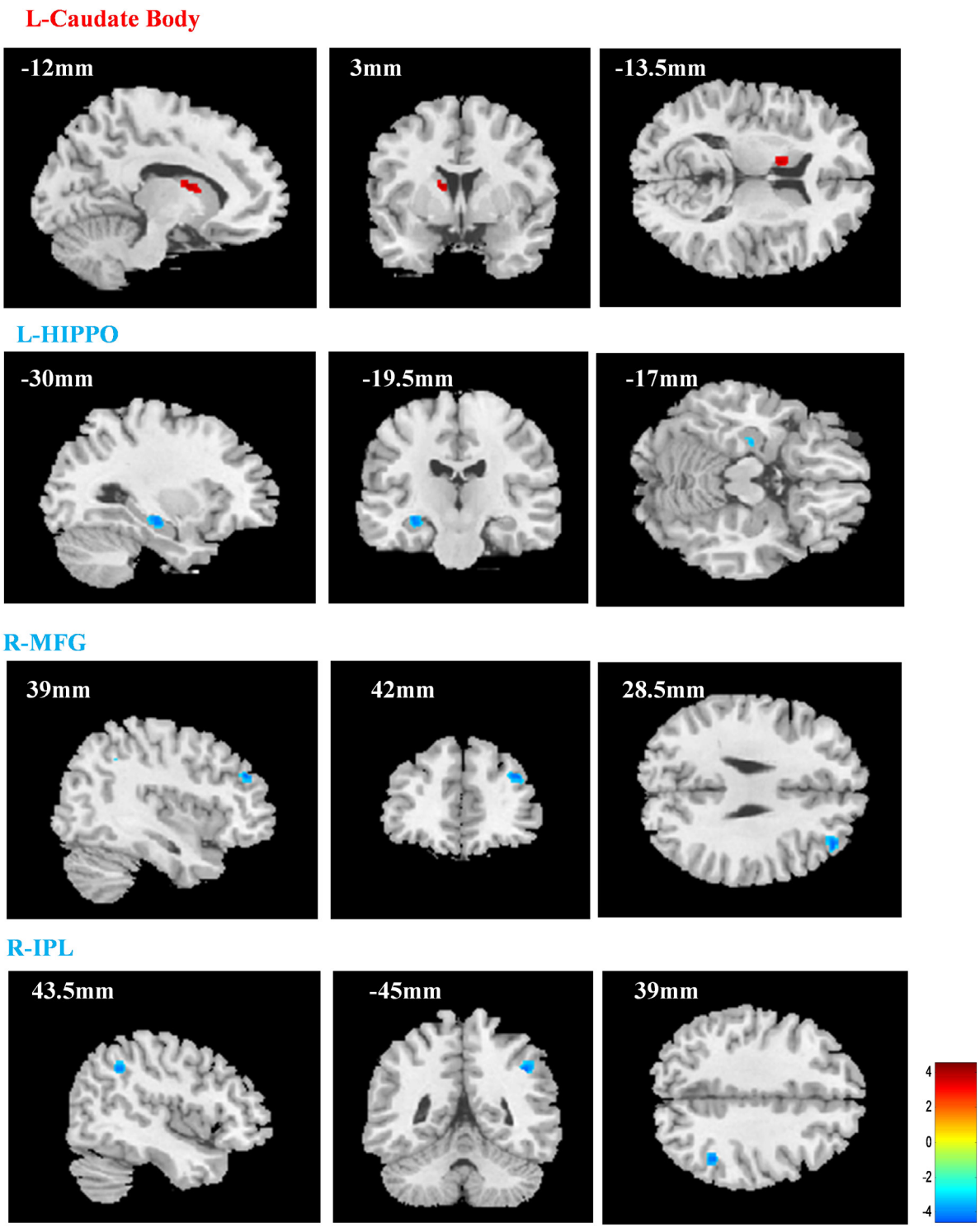

Figure 1. Regional GMV changes in subjects of exposure group compared with those of control group. Significantly increased GMV were seen in left caudate body (L-Caudate Body); significantly decreased areas were observed in the left hippocampus (L-HIPPO), the right middle frontal gyrus (R-MFG), and the right inferior parietal lobule (R-IPL). The red areas indicate high GMV brain regions and the blue areas indicate lower ones. The significance level was set at $p < 0.002$, $p < 0.05$ FDR corrected.

positively associated with DVBM accuracy (Figure 4B, $p = 0.0016$, $r = 0.434$) and DVIM accuracy (Figure 4C, $p = 0.0036$, $r = 0.4046$), respectively. What's more, as for the DVIM accuracy, we also found that it negatively associated with ReHo of the right superior frontal gyrus (Figure 4D, $p = 0.0178$, $r = -0.3362$) and the left amygdala (Figure 4E, $p = 0.0444$, $r = -0.2862$), respectively.

4. Discussion

Considering that the principal confounding factors were

Table 3. Regions showing significantly different GMV by comparing exposure and control group

Brain region	R/L	MNI coordinate (mm)			Volume (m^3)	Peak T value
		x	y	z		
Exposure < Control						
Hippocampus/Hippocampus_L (aal)	L	-30	-19.5	-17	151	-4.219
Middle Frontal Gyrus/Frontal_Mid_R (aal)	R	39	42	28.5	140	-4.373
Inferior Parietal Lobule/Parietal_Inf_R (aal)	R	43.5	-48	39	109	-4.377
Exposure < Control						
Caudate Body/Caudate_L (aal)	L	-12	3	13.5	131	3.715

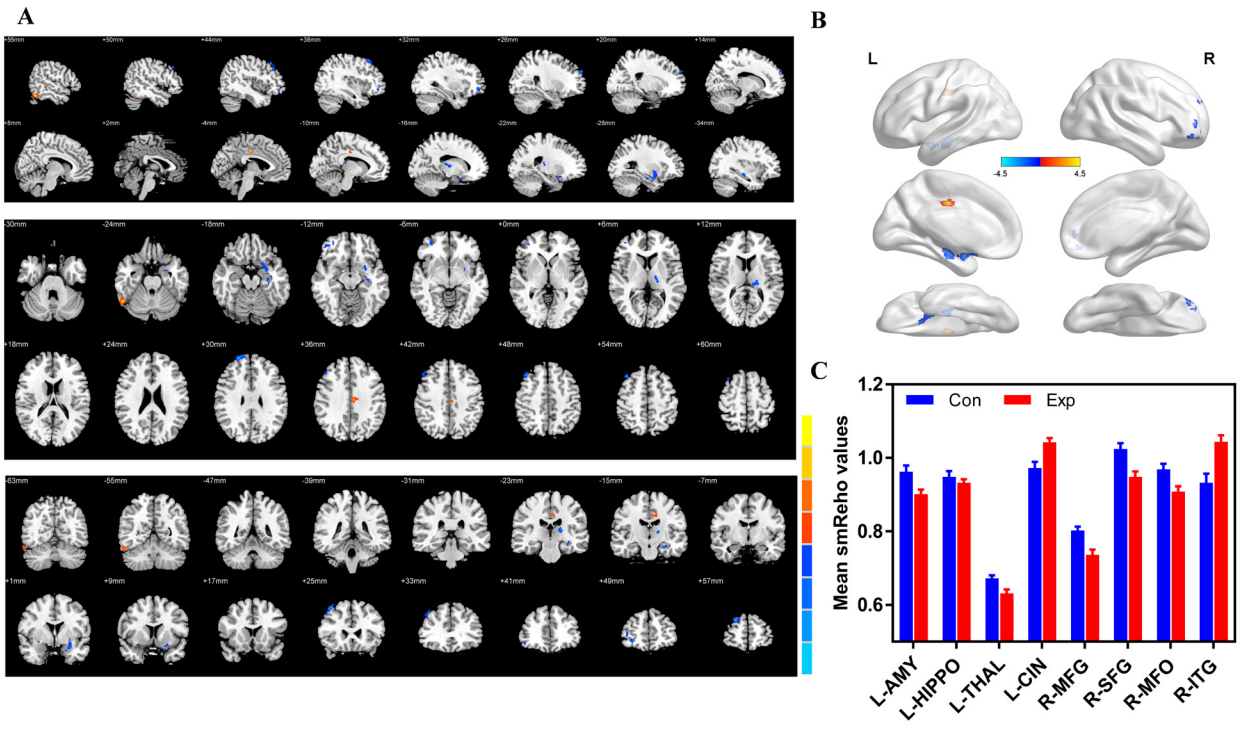

Figure 2. Regional ReHo value changes in subjects in exposure groups compared with control group. (A) MNI x,y,z plot and **(B)** BrainNet surface model shows that significantly increased areas were seen in Inferior Temporal Gyrus (R-ITG) and the left Cingulate Gyrus (L-CIN). Significantly decreased areas were observed in the left hippocampus (L-HIPPO), the left amygdala (L-AMY), the left thalamus (L-TH), the right middle frontal gyrus (R-MFG) and the right superior frontal gyrus (R-SFG). The red areas indicate high GMV brain regions and the blue areas indicate lower ones (*t*-test, $|t| > 2.70$, $p < 0.01$, AlphaSim corrected). **(C)** The mean smoothed ReHo values between the exposure and the control group subjects.

Table 4. Regions showing significantly different ReHo by comparing Control and Experiment group

Brain region	R/L	MNI coordinate (mm)			Volume (m^3)	Peak T value
		x	y	z		
Exposure < Control						
Amygdala/Amygdala_L (aal)	L	-28	0	-20	3645	-3.440
Hippocampus/Hippocampus_L (aal)	L	-32	-18	-12	1863	-3.369
Thalamus/Thalamus_L (aal)	L	-20	-20	12	2727	-3.369
Middle Frontal Gyrus/Frontal_Mid_R (aal)	R	42	28	50	4266	-4.108
Superior Frontal Gyrus/Frontal_Sup_R (aal)	R	24	58	30	2187	-4.021
Middle Frontal Gyrus/Frontal_Mid_Orb_R (aal)	R	32	48	-8	2592	-3.269
Exposure > Control						
Cingulate Gyrus/Cingulum_Mid_L (aal)	L	-6	-18	38	2160	4.118
Inferior Temporal Gyrus/Temporal_Inf_R (aal)	R	56	-58	-22	2727	4.082

Table 5. Regions showing significantly different ALFF/fALFF by comparing Control and Experiment group

Brain region	R/L	MNI coordinate (mm)			Volume (m^3)	Peak T value
		x	y	z		
ALFF						
Exposure < Control						
Superior Temporal Gyrus/Temporal_Sup_L (aal)	L	-46	-18	-20	149	-3.711
Hippocampus/Hippocampus_L (aal)	L	-28	2	-10	255	-4.561
Thalamus/Thalamus_L (aal)	L	-18	-24	10	200	-3.956
Exposure > Control						
Postcentral Gyrus/Postcentral_R (aal) (Brodmann area 6, 22, 42, 43)	R	62	-4	12	126	3.935
fALFF						
Exposure < Control						
Pons/Brainstem	-	-4	-18	-40	132	-4.940
Occipital Lobe/Occipital_Mid_L (aal)	L	-22	-68	16	150	-4.061
Middle Temporal Gyrus/Temporal_Mid_L (aal)	L	-48	-76	8	128	-3.761
Superior Frontal Gyrus/Frontal_Sup_L (aal)	L	-14	28	58	198	-4.786
Exposure > Control						
Cerebellum Posterior Lobe/Cerebelum_Crus1_R (aal)	R	26	-92	-30	218	4.316

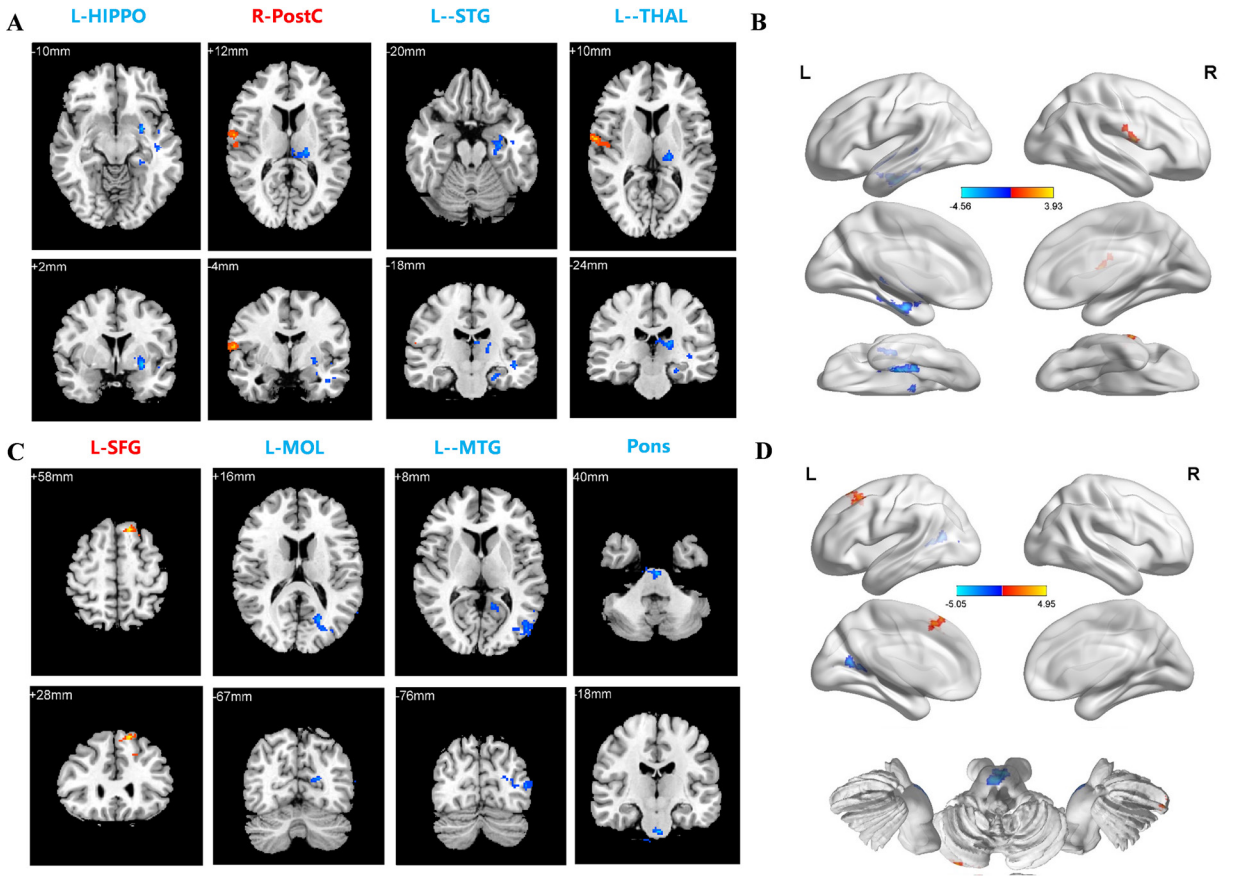

Figure 3. ALFF/fALFF signal changes in subjects in exposure group compared with control group. (A) MNI x,y,z plot and **(B)** BrainNet surface model showed that significantly decreased areas in ALFF analysis were found in the left superior temporal gyrus (L-STG), the left hippocampus (L-HIPPO) and the left thalamus (L-TH); And that significantly decreased areas in ALFF analysis were found in the postcentral gyrus (Brodmann area 6, 22, 42, 43). **(C)** MNI x,y,z plot and **(D)** BrainNet surface model showed that significantly decreased areas in fALFF analysis were found in Pons, the right occipital Lobe (L-MOL), and also the left middle temporal gyrus (L-MTG) and the superior frontal gyrus (L-STG); significantly increased areas in fALFF analysis were found in the cerebellum posterior lobe.

excluded from the study and that pilots and controls investigated were matched by age, working life and education status, the above-mentioned results suggest that exposure to aircraft noise in military pilots may lead to working memory impairment as well as brain structural and functional alteration.

In this study, we found that the DVBM and DVIM accuracies of military pilots were significantly lower than those of control military officers, indicating that long-term aircraft noise exposure may cast a detrimental

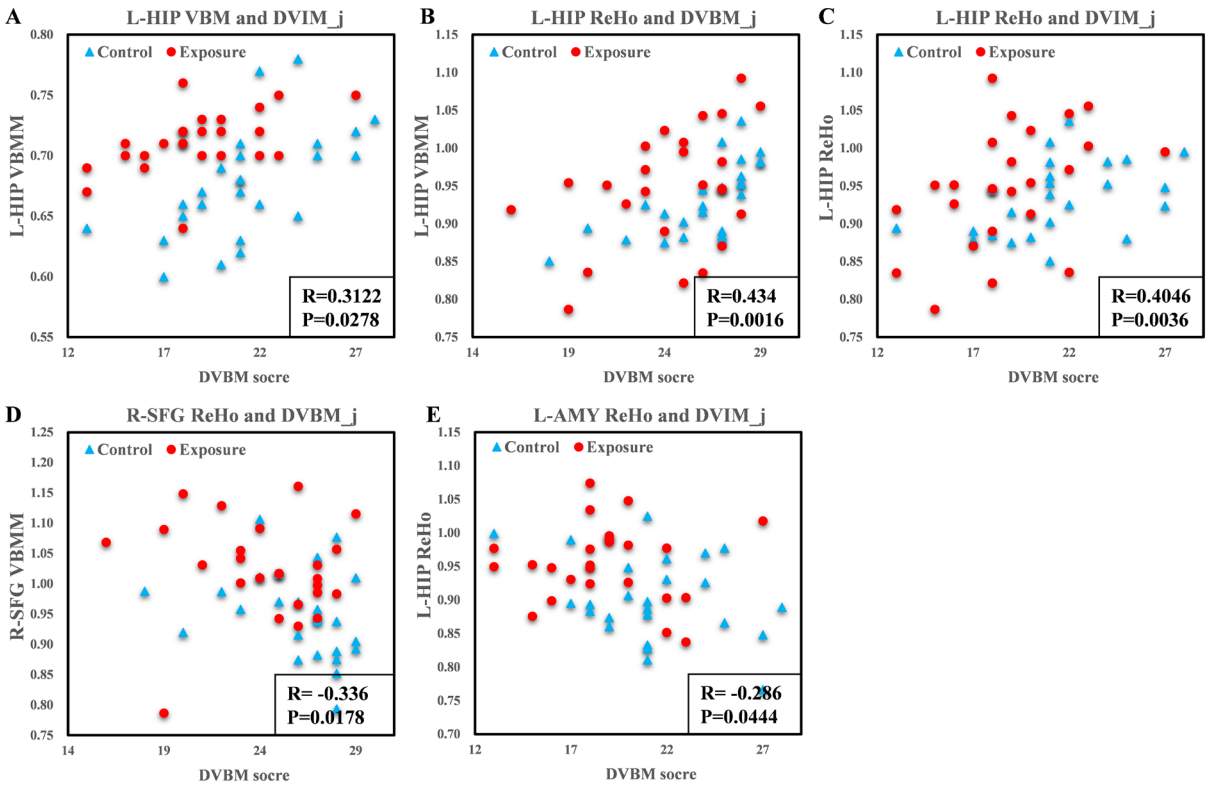

Figure 4. Scatterplots of significantly correlated DVBM/DVIM scores derived from the behavioral experiment against the neuroimaging parameters. (A) Scatterplot of DVIM scores against the GMV of left hippocampus (L-HIP). **(B)** Scatterplot of DVBM scores against the ReHo value of left hippocampus (L-HIP) **(C)** Scatterplot of DVIM scores against the ReHo value of left hippocampus (L-HIP) **(D)** Scatterplot of DVBM scores against the ReHo value of the right superior frontal gyrus (R-SFG). **(E)** Scatterplot of DVIM scores against the ReHo value of the left amygdala (L-AMY).

influence upon the working memory of humans. This result is consistent with earlier studies corroborating that noise exposure leads to memory impairment for both humans and non-human animals. Kempen *et al.* demonstrated that children attending schools with higher road or aircraft noise levels made significantly more errors in switching attention tests and digit memory span tests (*24*). Similarly, Loganathan *et al.* found an adverse effect of noise exposure on working memory in rodents exposed to simulated noise (*25*). Interestingly, significant differences between the two groups were only found in DVBM\DVIM tests rather than IVBM/IVIM tests. According to earlier studies, in the Munich Airport Study, Evans *et al.* found that children from noise exposed communities had more errors on a difficult subscale of German standardized reading tests than children from quiet communities; while the two groups did not differ on easy and intermediate portions of the test (*26*). Considering that DVBM\DVIM tests were more difficult than IVBM/IVIM, it can be concluded that performance on complex memory tasks is more susceptible to the effects of noise than performance on simple tasks.

By resting functional imaging analysis, we found decreased GMV, ReHo and ALFF in left hippocampi, indicating potential neuron loss and disrupted local functionality in these brain regions. Hippocampus is a medial temporal lobe structure which plays an important role in working memory (*27*). Adult hippocampal neurons are balanced by three main cellular events: cell proliferation, neuronal differentiation, and cell survival (*28*). According to previous studies, chronic hyperactivity of HPA-axis induced by noise stress can elevate the hippocampal corticosteroid receptors, lead to reduced hippocampal neurogenesis, cell proliferation, and impaired spatial memory in rodents (*29,30*). Besides, long-lasting elevated corticosterone levels also lead to increased apoptosis in the dentate gyrus of hippocampus, which has been shown in mice exposed to noise (*31*). Thus, we posit that neuron loss in hippocampi may be caused by reduced neurogenesis and proliferation as well as elevated cellular apoptosis under stress. Furthermore, noise exposure leads to abnormal synaptic plasticity in the structure and function of the hippocampus, temporal lobe, and amygdala. Noise also increases norepinephrine/noradrenaline (NE) and dopamine (DA) levels in hippocampus, while decreases serotonin 5 hydroxyindoleacetic acid (serotonin 5-HT) level (*32*). We inferred these alterations of synaptic plasticity and neurotransmitters may be contributing to the neural dysfunctionality in hippocampi we found in this study and lead to impaired learning and memory behavior.

The hippocampus is part of the limbic system, and plays important roles in the consolidation of information

from short-term memory to long-term memory, and in spatial memory that enables navigation (*27*). Neuron loss in hippocampus leads to memory impairment in aging and various neuropsychological disorders. For instance, previous VBM studies indicated that atrophy and neuron loss in hippocampus can significantly predict memory recall & storage performances in behavioral frontotemporal dementia, which is in accordance with our findings (*33*). Furthermore, similar to our results, decreased ReHo and ALFF in hippocampus were also observed in mild cognitive impairment patients compared to normal controls, which lead to increased errors in spatially-related memory tasks (*34*). Taken together, the structural and functional abnormalities noted in hippocampus in this study may be the key to working impairment under long-term aircraft noise exposure, which was further corroborated by the significant positive correlations between the DVBM\DVIM accuracies and the ReHo in the left hippocampus.

In this study, by resting functional imaging analysis, reduced neural activities were also found in left amygdala, left thalamus, left superior temporal gyrus and right superior/middle frontal gyrus. Amygdala, hippocampus, and frontal cortex are essential components of the neural circuitry mediating stress responses. The amygdala provides a primary association between subcortical areas, which are responsible for producing fear, and cerebral cortical areas receiving sensory information about the external environment (*35*). There is evidence of noise stress induced activation of the HPA-axis, amygdala, and other brain circuits and in producing abnormalities in timid and emotional or anxiety-like behaviors (*36*). Herein, we inferred that the functional alteration in these regions may be the result of HPA-axis hyperactivity.

In the meantime, we also found that the GMV of the left caudate body significantly increased in the exposure group. The basal ganglia have traditionally been viewed as motor processing nuclei; however, functional neuroimaging evidence has implicated these structures in more complex cognitive and affective processes that are fundamental for a range of human activities (*37*). In our analysis, however, the left caudate body GMV change did not correlate with the working memory score, suggesting that it may not function on working memory in cognitive function. Further research will discuss the possible relation of basal ganglia with other motor or cognitive function.

Interestingly, we found more noise induced neuron loss and neural dysfunction in left cerebrum, in comparison with the right side. Brain damage would be more likely to affect the left hemisphere in both childhood or adulthood, including epilepsy and stroke. According to radiological studies, there would be a biological basis for the higher vulnerability of the left hemisphere. The main pathogenetic factor seems to be a hemodynamic one, responsible for insufficient blood supply to the left hemisphere (*38*). The left hemisphere is also more vulnerable to traumatic stress and environmental stress. For example, Zhang *et al*. reported decreased GMV in the left hemisphere in flood disaster survivors with recent onset posttraumatic stress disorder (*39*), while Chen *et al*. observed both neuron loss and disrupted neural activities in the left hemisphere (rather than right hemisphere) after chronic hypoxia exposure (*10*), which is consistent with our results. We inferred that detrimental noise exposure may induce hemodynamic changes in the left hemisphere, and thus make it more vulnerable to the structural and functional abnormality.

Some limitations of the study must be recognized. First, like other population studies on noise stress, the neurobehavioral and neuroimaging findings in this study may be influenced by individual factors, ever-changing environments and co-exposure to other environmental pollutants or toxicants. To solve this problem, the potential confounding factors like age, work life and education status have been matched in the two groups. Besides, the subjects in exposure and control group were all enrolled from air force units and their education and work experience were quite similar to each other. A further study should be conducted to reveal the dose-effect relationship between the neurobehavioral impairment and neuroimaging abnormality. Second, the sample size of this study is relatively small, which should be expanded in future studies.

In conclusion, the current study demonstrates that long-term aircraft noise may lead to working memory impairment in jet fighter pilots. The hippocampus and other cognition region displayed both neuron loss and reduced local neural activities under chronic noise stress, which were further proved to be associated with neurobehavioral performance. Taken together, the detrimental impact of aircraft noise exposure on cognition should be considered in health maintenance of military pilots. A dysfunctional hippocampus may serve as structural and functional bases for neuropsychological impairment under exposure.

Acknowledgements

This study was financially supported by the National Science Foundation of China (No. 81470791, 81670594, 31770537).

References

1. Chen H, Kwong JC, Copes R, Tu K, Villeneuve PJ, van Donkelaar A, Hystad P, Martin RV, Murray BJ, Jessiman B, Wilton AS, Kopp A, Burnett RT. Living near major roads and the incidence of dementia, Parkinson's disease, and multiple sclerosis: A population-based cohort study. Lancet. 2017; 389:718-726.
2. van Kempen E, van Kamp I, Lebret E, Lammers J,

Emmen H, Stansfeld S. Neurobehavioral effects of transportation noise in primary schoolchildren: a cross-sectional study. Environ Health. 2010; 9:25.
3. Elmenhorst EM, Elmenhorst D, Wenzel J, Quehl J, Mueller U, Maass H, Vejvoda M, Basner M. Effects of nocturnal aircraft noise on cognitive performance in the following morning: Dose-response relationships in laboratory and field. Int Arch Occup Environ Health. 2010; 83:743-751.
4. Gordon B, Joachims Z, Cohen HB, Grossman A, Derazne E, Carmon E, Zilberberg M, Levy Y. Hearing loss in Israeli air force aviators: Natural history and risk factors. Mil Med. 2016; 181:687-692.
5. Jafari Z, Kolb BE, Mohajerani MH. Noise exposure accelerates the risk of cognitive impairment and Alzheimer's disease: Adulthood, gestational, and prenatal mechanistic evidence from animal studies. Neurosci Biobehav Rev. 2019. pii: S0149-7634(18)30897-2.
6. Burow A, Day HE, Campeau S. A detailed characterization of loud noise stress: Intensity analysis of hypothalamo-pituitary-adrenocortical axis and brain activation. Brain Res. 2005; 1062:63-73.
7. Rojas-Rueda D, Vrijheid M, Robinson O, Gunn Marit A, Grazuleviciene R, Slama R, Nieuwenhuijsen M. Environmental burden of childhood disease in Europe. Int J Environ Res Public Health. 2019; 16. pii: E1084.
8. Jafari Z, Kolb BE, Mohajerani MH. Chronic traffic noise stress accelerates brain impairment and cognitive decline in mice. Exp Neurol. 2018; 308:1-12.
9. Kim JJ, Lee HJ, Welday AC, Song E, Cho J, Sharp PE, Jung MW, Blair HT. Stress-induced alterations in hippocampal plasticity, place cells, and spatial memory. Proc Natl Acad Sci U S A. 2007; 104:18297-18302.
10. Chen X, Zhang Q, Wang J, *et al*. Cognitive and neuroimaging changes in healthy immigrants upon relocation to a high altitude: A panel study. Hu Hum Brain Mapp. 2017; 38:3865-3877.
11. Littleton AC, Register-Mihalik JK, Guskiewicz KM. Test-retest reliability of a computerized concussion test: CNS vital signs. Sports Health. 2015; 7:443-447.
12. Gualtieri CT, Johnson LG. Reliability and validity of a computerized neurocognitive test battery, CNS vital Signs. Arch Clin Neuropsychol. 2006; 21:623-643.
13. Matsuda H, Mizumura S, Nemoto K, Yamashita F, Imabayashi E, Sato N, Asada T. Automatic voxel-based morphometry of structural MRI by SPM8 plus diffeomorphic anatomic registration through exponentiated lie algebra improves the diagnosis of probable Alzheimer Disease. AJNR Am J Neuroradiol. 2012; 33:1109-1114.
14. Kim GW, Kim YH, Jeong GW. Whole brain volume changes and its correlation with clinical symptom severity in patients with schizophrenia: A DARTEL-based VBM study. PloS One. 2017; 12:e0177251.
15. Chen Z, Li L, Sun J, Ma L. Mapping the brain in type II diabetes: Voxel-based morphometry using DARTEL. Eur J Radiol. 2012; 81:1870-1876.
16. Yu E, Liao Z, Tan Y, Qiu Y, Zhu J, Han Z, Wang J, Wang X, Wang H, Chen Y, Zhang Q, Li Y, Mao D, Ding Z. High-sensitivity neuroimaging biomarkers for the identification of amnestic mild cognitive impairment based on resting-state fMRI and a triple network model. Brain Imaging Behav. 2019; 13:1-14.
17. Chao-Gan Y, Yu-Feng Z. DPARSF: A MATLAB toolbox for "Pipeline" data analysis of resting-state fMRI. Front Syst Neurosci. 2010; 4:13.
18. Cordova-Palomera A, Tornador C, Falcon C, Bargallo N, Nenadic I, Deco G, Fananas L. Altered amygdalar resting-state connectivity in depression is explained by both genes and environment. Hum Brain Mapp. 2015; 36:3761-3776.
19. Foster GE, Davies-Thompson J, Dominelli PB, Heran MK, Donnelly J, duManoir GR, Ainslie PN, Rauscher A, Sheel AW. Changes in cerebral vascular reactivity and structure following prolonged exposure to high altitude in humans. Physiol Rep. 2015; 3. pii: e12647.
20. Yan CG, Wang XD, Zuo XN, Zang YF. DPABI: Data processing & analysis for (resting-state) brain imaging. Neuroinformatics. 2016; 14:339-351.
21. Zou QH, Zhu CZ, Yang Y, Zuo XN, Long XY, Cao QJ, Wang YF, Zang YF. An improved approach to detection of amplitude of low-frequency fluctuation (ALFF) for resting-state fMRI: fractional ALFF. J Neurosci Methods. 2008; 172:137-141.
22. Cantou P, Platel H, Desgranges B, Groussard M. How motor, cognitive and musical expertise shapes the brain: Focus on fMRI and EEG resting-state functional connectivity. J Chem Neuroanat. 2018; 89:60-68.
23. Li Z, Kadivar A, Pluta J, Dunlop J, Wang Z. Test-retest stability analysis of resting brain activity revealed by blood oxygen level-dependent functional MRI. J Magn Reson Imaging. 2012; 36:344-354.
24. van Kempen EE, van Kamp I, Stellato RK, Lopez-Barrio I, Haines MM, Nilsson ME, Clark C, Houthuijs D, Brunekreef B, Berglund B, Stansfeld SA. Children's annoyance reactions to aircraft and road traffic noise. J Acoust Soc Am. 2009; 125:895-904.
25. Loganathan S, Rathinasamy S. Alteration in memory and electroencephalogram waves with sub-acute noise stress in albino rats and safeguarded by scoparia dulcis. Pharmacogn Mag. 2016; 12:S7-s13.
26. Bullinger M, Hygge S, Evans GW, Meis M, von Mackensen S. The psychological cost of aircraft noise for children. Zentralbl Hyg Umweltmed. 1999; 202:127-138.
27. Knierim JJ. The hippocampus. Curr Biol. 2015; 25:R1116-1121.
28. Kempermann G. Activity dependency and aging in the regulation of adult neurogenesis. Cold Spring Harb Perspect Biol. 2015; 7. pii: a018929.
29. Henckens MJ, van der Marel K, van der Toorn A, Pillai AG, Fernandez G, Dijkhuizen RM, Joels M. Stress-induced alterations in large-scale functional networks of the rodent brain. NeuroImage. 2015; 105:312-322.
30. Hu L, Yang J, Song T, Hou N, Liu Y, Zhao X, Zhang D, Wang L, Wang T, Huang C. A new stress model, a scream sound, alters learning and monoamine levels in rat brain. Physiol Behav. 2014; 123:105-113.
31. Gonzalez-Perez O, Chavez-Casillas O, Jauregui-Huerta F, Lopez-Virgen V, Guzman-Muniz J, Moy-Lopez N, Gonzalez-Castaneda RE, Luquin S. Stress by noise produces differential effects on the proliferation rate of radial astrocytes and survival of neuroblasts in the adult subgranular zone. Neurosci Res. 2011; 70:243-250.
32. Ravindran R, Rathinasamy SD, Samson J, Senthilvelan M. Noise-stress-induced brain neurotransmitter changes and the effect of Ocimum sanctum (Linn) treatment in albino rats. J Pharmacol Sci. 2005; 98:354-360.
33. Bertoux M, Flanagan EC, Hobbs M, Ruiz-Tagle A, Delgado C, Miranda M, Ibanez A, Slachevsky A, Hornberger M. Structural anatomical investigation of

long-term memory deficit in behavioral frontotemporal dementia. J Alzheimers Dis. 2018; 62:1887-1900.
34. Qing Z, Li W, Nedelska Z, Wu W, Wang F, Liu R, Zhao H, Chen W, Chan Q, Zhu B, Xu Y, Hort J, Zhang B. Spatial navigation impairment is associated with alterations in subcortical intrinsic activity in mild cognitive impairment: A resting-state fMRI study. Behav Neurol. 2017; 2017:6364314.
35. Wilson MA, Grillo CA, Fadel JR, Reagan LP. Stress as a one-armed bandit: Differential effects of stress paradigms on the morphology, neurochemistry and behavior in the rodent amygdala. Neurobiol Stress. 2015; 1:195-208.
36. Jafari Z, Mehla J, Kolb BE, Mohajerani MH. Prenatal noise stress impairs HPA axis and cognitive performance in mice. Sci Rep. 2017; 7:10560.
37. Arsalidou M, Duerden EG, Taylor MJ. The centre of the brain: Topographical model of motor, cognitive, affective, and somatosensory functions of the basal ganglia. Hum Brain Mapp. 2013; 34:3031-3054.
38. Taylor DC. Differential rates of cerebral maturation between sexes and between hemispheres. Evidence from epilepsy. Lancet. 1969; 2:140-142.
39. Zhang J, Tan Q, Yin H, Zhang X, Huan Y, Tang L, Wang H, Xu J, Li L. Decreased gray matter volume in the left hippocampus and bilateral calcarine cortex in coal mine flood disaster survivors with recent onset PTSD. Psychiatry Res. 2011; 192:84-90.

(Received July 22, 2019; Revised September 12, 2019; Accepted September 23, 2019)